

Multistep Inhibition of α -Synuclein Aggregation and Toxicity *in Vitro* and *in Vivo* by Trodusquemine

Michele Perni,^{†,‡,+,ID} Patrick Flagmeier,^{†,‡,+,ID} Ryan Limbocker,^{†,‡,+,ID} Roberta Cascella,[§] Francesco A. Aprile,^{†,‡,ID} Céline Galvagnion,^{†,||,ID} Gabriella T. Heller,^{†,‡,+,ID} Georg Meisl,^{†,‡,ID} Serene W. Chen,^{†,‡,ID} Janet R. Kumita,^{†,‡,ID} Pavan K. Challa,^{†,‡,ID} Julius B. Kirkegaard,[⊥] Samuel I. A. Cohen,^{†,‡} Benedetta Mannini,^{†,‡} Denise Barbut,[#] Ellen A. A. Nollen,[∇] Cristina Cecchi,[§] Nunilo Cremades,[○] Tuomas P. J. Knowles,^{†,‡,◆,ID} Fabrizio Chiti,^{*,§,ID} Michael Zasloff,^{*,#,¶,ID} Michele Vendruscolo,^{*,†,‡,ID} and Christopher M. Dobson^{*,†,‡}

[†]Department of Chemistry, University of Cambridge, Cambridge CB2 1EW, United Kingdom

[‡]Centre for Misfolding Diseases, Department of Chemistry, University of Cambridge, Cambridge CB2 1EW, United Kingdom

[§]Department of Experimental and Clinical Biomedical Sciences, University of Florence, Florence 50134, Italy

^{||}German Centre for Neurodegenerative Diseases, DZNE, Sigmund-Freud-Strasse. 27, 53127, Bonn, Germany

[⊥]Department of Applied Mathematics and Theoretical Physics, University of Cambridge, Cambridge CB3 0WA, United Kingdom

[#]Enterin Inc., 3624 Market Street, Philadelphia, Pennsylvania 19104, United States

[∇]University Medical Centre Groningen, European Research Institute for the Biology of Aging, University of Groningen, Groningen 9713 AV, The Netherlands

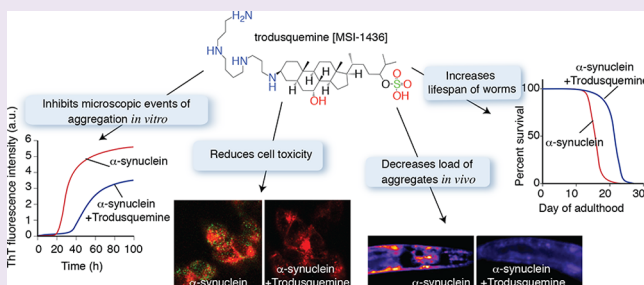
[○]Biocomputation and Complex Systems, Physics Institute (BIFI)-Joint Unit BIFI-IQFR (CSIC), University of Zaragoza, 50018 Zaragoza, Spain

[◆]Department of Physics, Cavendish Laboratory, University of Cambridge, Cambridge CB3 0HE, United Kingdom

[¶]MedStar-Georgetown Transplant Institute, Georgetown University School of Medicine, Washington, DC 20010, United States

Supporting Information

ABSTRACT: The aggregation of α -synuclein, an intrinsically disordered protein that is highly abundant in neurons, is closely associated with the onset and progression of Parkinson's disease. We have shown previously that the aminosterol squalamine can inhibit the lipid induced initiation process in the aggregation of α -synuclein, and we report here that the related compound trodusquemine is capable of inhibiting not only this process but also the fibril-dependent secondary pathways in the aggregation reaction. We further demonstrate that trodusquemine can effectively suppress the toxicity of α -synuclein oligomers in neuronal cells, and that its administration, even after the initial growth phase, leads to a dramatic reduction in the number of α -synuclein inclusions in a *Caenorhabditis elegans* model of Parkinson's disease, eliminates the related muscle paralysis, and increases lifespan. On the basis of these findings, we show that trodusquemine is able to inhibit multiple events in the aggregation process of α -synuclein and hence to provide important information about the link between such events and neurodegeneration, as it is initiated and progresses. We suggest, in addition, that trodusquemine has the potential to be a therapeutic candidate in Parkinson's disease and related disorders, for these effects as well for its ability to cross the blood–brain barrier and promote tissue regeneration.



The aggregation of α -synuclein, a 140-residue protein highly expressed in neuronal synapses,^{1–5} is a hallmark of the pathogenesis of a variety of neurodegenerative disorders collectively known as α -synucleinopathies, including Parkinson's disease (PD), PD with dementia, dementia with Lewy bodies, and multiple-system atrophy.^{5–12} The mechanism of aggregation of α -synuclein is highly complex and is modulated by a variety of environmental factors, such as pH, temperature, ionic strength, and the presence of cosolvents, and by its interactions with a range of cellular

components, including lipid membranes.^{13–20} In addition, the aggregation process is highly heterogeneous and leads to the formation of multiple types of fibrillar and prefibrillar species, the degree of polymorphism of which also depends on the experimental conditions.^{21–26}

Received: May 18, 2018

Accepted: June 4, 2018

53 Although it is challenging to study the mechanistic events asso-
54 ciated with α -synuclein aggregation, a detailed understanding of
55 this process is of considerable importance for the rational devel-
56 opment and evaluation of potential therapeutics directed at
57 reducing or eliminating the underlying sources of toxicity that
58 lead to PD.^{10,27–29} The aggregation of α -synuclein has been
59 shown to be enhanced dramatically by its binding to lipid mem-
60 branes;^{14,30} disrupting such interactions with small molecules
61 therefore, has the potential to provide new information about the
62 molecular processes involved in pathogenicity and could also
63 represent the basis for an effective therapeutic strategy. In this con-
64 text, we have recently found that the aminosterol squalamine^{31–33}
65 interferes with the binding of α -synuclein to membranes, reduces
66 the initiation of its aggregation *in vitro*, and decreases the toxicity
67 associated with such aggregation in human neuroblastoma cells
68 and in a *C. elegans* model of PD.²⁹

69 The existence of additional natural aminosterol compounds
70 related to squalamine³³ prompted us to explore their effects on
71 the formation and properties of α -synuclein aggregates *in vitro*
72 and *in vivo*. One such compound, trodusquemine (also known as
73 MSI-1436, Figure S1a),^{32–34} belongs to a class of cationic amphi-
74 pathic aminosterols that have been widely studied in both animal
75 models and in clinical trials in relation to the treatment of
76 cancer,³⁵ anxiety,³⁶ and obesity.^{37,38} Trodusquemine was initially
77 isolated from dogfish shark liver as a minor aminosterol along
78 with six other related compounds, including squalamine.³³ More-
79 over, it has since been shown to be able to cross the blood–brain
80 barrier, a property of considerable importance for any therapeutic
81 molecule for the treatment of neuropathic disorders.³¹ In addition,
82 trodusquemine has been shown to be able to stimulate regener-
83 ation in a range of vertebrate tissues and organs following injury
84 with no apparent effect on uninjured tissues.³⁹ Trodusquemine
85 shares the same parent structure as squalamine, but with a
86 spermine moiety replacing the spermidine on the side chain,
87 resulting in an increased positive charge (Figure S1a).

88 Given the structural similarity between trodusquemine and
89 squalamine, and previous reports suggesting that the more posi-
90 tively charged trodusquemine is likely to enhance its ability to
91 reduce negative electrostatic surface charges on intracellular mem-
92 branes,^{32,40} we set out to characterize the effects of trodusquemine
93 on the aggregation kinetics of α -synuclein *in vitro* using experi-
94 mental conditions previously used to study individual micro-
95 scopic steps in the aggregation of α -synuclein in the absence of
96 any aminosterol.^{15,41}

97 Our first studies of the effects of trodusquemine presented here
98 were aimed to probe its effects on the initiation of α -synuclein
99 aggregation in the presence of lipid vesicles,^{14,15,30,41} on fibril
100 elongation,^{13,15,41} and on secondary nucleation.^{13,15,41,42} We then
101 explored the effects of trodusquemine on inhibiting the cyto-
102 toxicity of preformed oligomers of α -synuclein toward neuronal
103 cells.⁴³ We also evaluated the effects of trodusquemine using a
104 well-established transgenic *C. elegans* model of PD, in which
105 α -synuclein forms inclusions over time in the large muscle cells
106 leading to age-dependent paralysis.²⁹

107 ■ RESULTS AND DISCUSSION

108 **Trodusquemine Inhibits Both the Lipid-Induced**
109 **Initiation and the Fibril-Induced Amplification Steps of**
110 **α -Synuclein Aggregation.** In order to characterize systemati-
111 cally the influence of trodusquemine on the microscopic events
112 involved in the aggregation of α -synuclein, we employed a
113 previously described three-pronged chemical kinetics strat-
114 egy.^{13,15,41,42} This approach involves the study of α -synuclein

aggregation under a series of specifically designed conditions that
make it possible to characterize separately the processes of hetero-
geneous primary nucleation,¹⁴ fibril elongation,^{13,15,41,42} and fibril
amplification,^{13,15,41,42} the latter including secondary processes
such as fragmentation and surface-catalyzed secondary nucleation
that result in the proliferation of aggregated forms of α -synuclein.

First, we tested the influence of trodusquemine on the lipid-
induced initiation of α -synuclein aggregation.^{14,15} Using DMPS
vesicles at 30 °C,¹⁴ we observed that increasing concentrations of
trodusquemine resulted in an increase in the diameter of the
vesicles to above 100 nm for trodusquemine-to-lipid ratios above
0.2, as monitored by dynamic light scattering (Figure S2a).
We have shown previously that variations in the size of the
vesicles below 100 nm does not affect the kinetics of aggregation
of α -synuclein,¹⁴ and so in the present study we carried out all
kinetic and lipid-binding experiments at trodusquemine-to-lipid
ratios below 0.2. α -Synuclein was therefore incubated at a variety
of concentrations, ranging from 20 to 100 μ M, in the presence of
100 μ M DMPS under quiescent conditions at 30 °C, and in the
presence of concentrations of trodusquemine ranging from 0 to
10 μ M. The aggregation reaction was monitored in real time
using ThT fluorescence (Figures S3 and S4), and we observed a
dose-dependent inhibition of the lipid-induced aggregation of
 α -synuclein by trodusquemine, which was very similar to that
observed in the presence of squalamine.²⁹

In light of these results, we investigated the influence of
trodusquemine on the lipid-binding properties of α -synuclein
using far-UV circular dichroism (CD) spectroscopy. We incu-
bated 5 μ M α -synuclein in the presence of 250 μ M DMPS
and increasing concentrations of trodusquemine (0–50 μ M;
Figure S2b,c). At the protein-to-lipid ratio used in these experi-
ments, effectively all the protein molecules in the absence of
trodusquemine are bound to the surface of DMPS vesicles in an
 α -helical conformation, as predicted from the binding constants
previously determined for the α -synuclein-DMPS system¹⁴
(Figure S2b). In the presence of increasing concentrations of
trodusquemine, the CD signal of α -synuclein measured at
222 nm increases from a value characteristic of an α -helix to that
of a random coil (Figure S2c), indicating that trodusquemine,
like squalamine, can displace α -synuclein from the surfaces of
vesicles.

We then analyzed these data using the competitive binding
model that was used to describe the displacement of α -synuclein
from vesicles by β -synuclein^{13,15,41} and by squalamine,²⁹ in which
 α -synuclein and β -synuclein or squalamine compete for binding
sites at the surface of the DMPS vesicles. This analysis allowed us
to determine both the dissociation constant ($K_{D,T}$) and stoichi-
ometry (L_T) associated with the trodusquemine–DMPS system,
 $K_{D,T} = 1.62 \times 10^{-8}$ M and $L_T = 5.1$ (Figure S2c). In comparable
experiments conducted with the squalamine–DMPS system, we
found $K_{D,S} = 6.7 \times 10^{-8}$ M and $L_S = 7.3$, respectively;²⁹ the higher
affinity for the anionic phospholipids by trodusquemine
compared to squalamine is expected on the basis of the higher
net positive charge of the former zwitterion. To characterize this
inhibition in more detail, we analyzed the early time points of the
aggregation reaction (see Materials and Methods for details) by
globally fitting a single-step nucleation model to the kinetic traces
as previously described for squalamine¹⁴ (Figures 1a,b, S4 and S5).
This analysis is described in the Supporting Information (SI) and
indicates that trodusquemine inhibits α -synuclein lipid induced
aggregation *via* a somewhat more complex mechanism than
that reported for squalamine. In particular, our analysis suggests
that the mechanism involves not only the displacement of

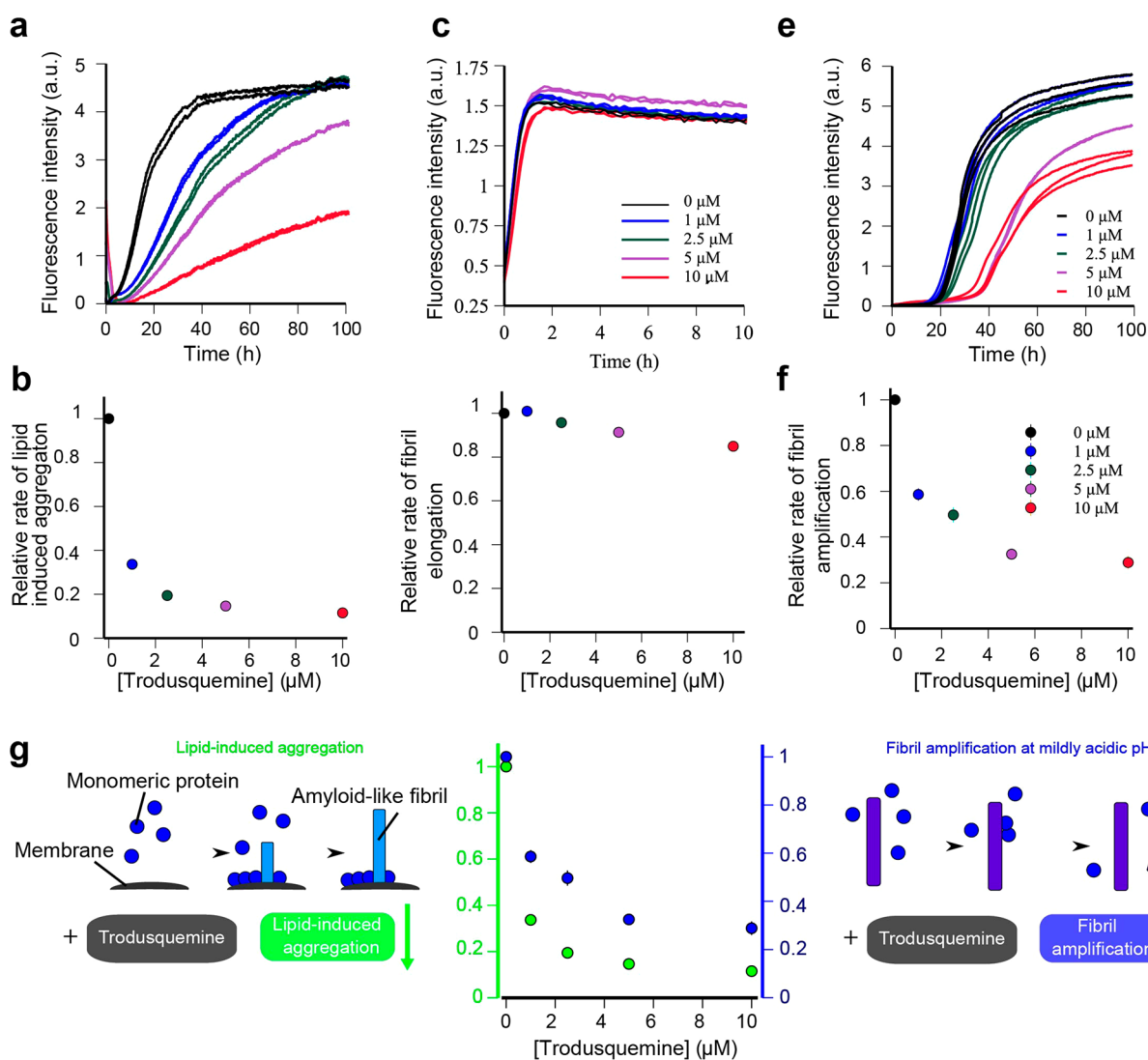


Figure 1. Inhibition of both the lipid-induced initiation and the fibril-induced amplification steps in α -synuclein aggregation *in vitro* by trodusquemine. (a) Change in ThT fluorescence intensity when 100 μ M monomeric α -synuclein was incubated in the presence of 100 μ M DMPS vesicles and 50 μ M ThT in 20 mM phosphate buffer (pH 6.5) under quiescent conditions at 30 $^{\circ}$ C. Trodusquemine was added to the solutions at increasing concentrations (black, 0 μ M; dark blue, 1 μ M; green, 2.5 μ M; purple, 5 μ M; red, 10 μ M); two independent traces are shown for each concentration. (b) Relative rates of lipid-induced aggregation. The data were analyzed by globally fitting the early times of the kinetic traces using a single-step nucleation model^{15,41} (see **Materials and Methods** for details). (c) Change in ThT fluorescence intensity when 100 μ M monomeric α -synuclein was incubated in the presence of 5 μ M preformed fibrils (monomer equivalents) and 50 μ M ThT in 20 mM phosphate buffer (pH 6.5) under quiescent conditions at 37 $^{\circ}$ C. Increasing concentrations of trodusquemine were added to the solution (colors as in panel a), and two independent traces are shown for each concentration. (d) Effects of trodusquemine on the relative rates of fibril elongation. The rates of elongation were extracted through linear fits to the early time points of the kinetic traces shown in c.^{13,15,41} (e) Change in ThT fluorescence when 100 μ M monomeric α -synuclein was incubated in the presence of 50 nM preformed fibrils and 50 μ M ThT in 20 mM phosphate buffer (pH 4.8) at 37 $^{\circ}$ C under quiescent conditions. Trodusquemine was added at different concentrations (colors as in panel a); two independent traces are shown for each concentration. (f) Effects of trodusquemine on the relative rates of fibril amplification. The rates were analyzed by determining the change in fibril number concentration at the half time of the aggregation reaction.^{15,41} (g) Schematic representation of the effects of trodusquemine on lipid-induced aggregation and fibril amplification.

178 monomeric α -synuclein from the membrane, as observed for
179 squalamine, but also the interaction with intermediate species on
180 the aggregation pathway; indeed, such interactions could also
181 contribute to the ability of trodusquemine to suppress the inter-
182 action of α -synuclein oligomers with cell membranes as described
183 below.

184 We next explored the influence of trodusquemine on fibril
185 elongation and secondary nucleation using experiments carried
186 out in the presence of preformed fibrils at neutral and acidic
187 pH.^{13,15,41} We studied fibril elongation by performing experi-
188 ments with monomeric α -synuclein (20–100 μ M) in the presence
189 of preformed fibrils of the protein at a concentration of 5 μ M

(monomer equivalents) under quiescent conditions at pH 6.5
190 and 37 $^{\circ}$ C (Figures 1c and S6); under these conditions, the
191 kinetics of α -synuclein aggregation have been found to be domi-
192 nated by the rate of fibril elongation.^{13,15} The kinetic profiles of
193 the aggregation reaction were then acquired in the presence of
194 various concentrations of trodusquemine [0–10 μ M]. In all
195 cases, the ThT fluorescence was found to decrease slowly during
196 the apparent plateau reached at the end of the reaction. This
197 behavior is often observed in such measurements, primarily
198 because fibrils formed during the reaction tend to assemble into
199 large assemblies with reduced exposed surface area available for
200 ThT interaction.^{13,15,41} For each trodusquemine concentration, 201

we extracted the elongation rate through linear fits of the early time points of the kinetic traces^{13,15} and found that trodusquemine does not detectably influence fibril elongation (Figures 1d and S7). We then explored the influence of trodusquemine on fibril-catalyzed secondary nucleation by incubating monomeric α -synuclein (60–100 μM) at 37 °C in the presence of preformed fibrils at a concentration of 50 nM (monomer equivalents) with increasing concentrations of trodusquemine (0–10 μM) under quiescent conditions at pH 4.8^{13,15,41} (Figures 1e,f, S8, S9). We then analyzed the change in fibril number concentration as previously described¹⁵ and found that the rate of secondary nucleation decreased significantly with increasing concentrations of trodusquemine.

The observation that trodusquemine can inhibit secondary nucleation processes is likely to be associated with its ability to bind to the surfaces of amyloid fibrils, as such a situation has been found for molecular chaperones that show similar abilities.⁴⁴ We therefore probed the binding of trodusquemine to α -synuclein fibrils by incubating preformed fibrils at a concentration of 10 μM (monomer equivalents) overnight with equimolar concentrations of trodusquemine, followed by an ultracentrifugation step.²⁹ We determined the concentration of trodusquemine in the supernatant before and after incubation with fibrils using mass spectrometry (Figure S10) and found that approximately 70% of the trodusquemine molecules were associated with the fibrils, consistent with its ability to bind to their surfaces and inhibit the secondary nucleation of α -synuclein. In summary, therefore, we observed that trodusquemine inhibits both the lipid-induced initiation and the fibril-induced amplification (secondary nucleation) step, in the process of α -synuclein aggregation (Figure 1g). This behavior can be attributed, at least in large part, to its ability to displace the protein from the surface of both lipid vesicles and fibrils.

In order to exclude the probability that any contribution to the observed effects was a result of the quenching of ThT by trodusquemine, we incubated preformed α -synuclein fibrils with ThT in the presence or absence of trodusquemine and could see that the compound did not affect the ThT signal to any detectable extent (Figure S11). In addition, because it has been found in some cases that a small molecule can inhibit the aggregation by sequestering proteins in a nonspecific manner as micelles or larger aggregates,⁴⁵ we investigated the behavior of trodusquemine itself under the conditions used here (20 mM phosphate buffer, pH 6.5, 30 °C), using 1D ¹H and 2D ¹H diffusion ordered spectroscopy (DOSY) experiments (Figures S12 and S13). The comparison of the trodusquemine intensities with those of an internal standard with the same concentration indicated that trodusquemine is very largely (>95%) monomeric under these conditions (Figure S12). Moreover, a diffusion coefficient of $2.42 \times 10^{-10} \text{ m}^2 \text{ s}^{-1}$, which is typical of a small molecule of this size in an aqueous solution, was determined for trodusquemine under these conditions, ruling out its self-assembly in solution (Figure S13). This result is supported by the absence of significant effects in the elongation step described above (Figure 1), which would be decreased if the concentration of free monomeric trodusquemine were reduced.

Trodusquemine Suppresses the Toxicity of α -Synuclein Oligomers in Human Neuroblastoma Cells by Inhibiting Their Binding to the Cell Membrane. In an additional series of experiments, we explored the effect of trodusquemine on the cytotoxicity associated with the aggregation of α -synuclein.^{43,46,47} We prepared samples of toxic type B* oligomers based on recently developed protocols^{46,47} and added them

to the cell culture medium of human Sh-Sy5Y neuroblastoma cells at a concentration of 0.3 μM (monomer equivalents of α -synuclein). The MTT assay, which provides a measure of cellular viability (see Methods for details), confirms previous results that these oligomers are toxic to cells (Figure 2a). We then treated the cells with these oligomers (0.3 μM) in the presence of increasing concentrations of trodusquemine (0.03, 0.1, and 0.3 μM) and observed that the toxicity was markedly reduced, particularly at the highest trodusquemine concentration (0.3 μM) where essentially complete protection was observed (Figure 2a). In addition, these α -synuclein oligomers (0.3 μM) in the absence of trodusquemine were shown to induce an increase in the levels of reactive oxygen species (ROS) in this cell model, indicating their ability to inflict cellular damage (Figure 2b). Repeating the experiments with increasing concentrations of trodusquemine (0.03, 0.3, and 3.0 μM), however, resulted in a marked decrease in the degree of ROS-derived fluorescence, showing a well-defined dose dependence and virtually complete inhibition of intracellular ROS production at a protein-to-trodusquemine ratio of 1:10 (Figure 2b).

We next investigated the mechanism by which trodusquemine inhibits α -synuclein oligomer toxicity by probing the interactions between the oligomers (0.3 μM) and human SH-SY5Y cells at increasing concentrations of trodusquemine (0.03, 0.3, and 3.0 μM) using anti- α -synuclein antibodies in conjunction with confocal microscopy. The images were scanned at apical planes to detect oligomers (green) interacting with cellular surfaces (red) by confocal microscopy (Figure 2c). Following the addition of the α -synuclein oligomers to the cell culture medium, a large number of these species were observed to be associated with the plasma membranes of the cells, but their number was significantly and progressively decreased as the trodusquemine concentration was increased, showing a well-defined dose dependence (Figure 2c). We have shown previously that the toxicity caused by protein oligomers, which are membrane disruptive,^{43,48,49} correlates with the affinity of membrane binding.⁵⁰ This protective effect can therefore be attributed to the reduced ability of α -synuclein oligomers to interact with the cell membranes in the presence of trodusquemine. Such protection is likely to result from the ability of trodusquemine to bind to the cellular membranes and displace the oligomers from them, and potentially through its interactions with the oligomeric species themselves as suggested by the *in vitro* experiments on lipid binding discussed above.

Trodusquemine Inhibits Formation of the α -Synuclein Inclusion in a *C. elegans* Model of PD and Increases Both Fitness and Longevity of the PD Worms. To examine whether or not trodusquemine shows the effects observed in cell cultures in a living organism, we used a well-established *C. elegans* model in which α -synuclein is overexpressed in the large muscle cells (“PD worms”) that shows age-dependent inclusion formation and related toxicity, which can be measured by a decrease in the number of body bends per minute (BPM), an increase in paralysis rate, and a decrease in the speed of movement.²⁹ As described previously for squalamine, we first carried out experiments aimed at optimizing the treatment profile of the worms.²⁹ We evaluated different treatment schedules by administering trodusquemine as a single, continuous dose either at an early stage of the life of the animals (L4 larval stage) or late in adulthood (D5, adulthood stage; Figure 3a).

We then investigated PD worms expressing α -synuclein fused to the yellow fluorescent protein (YFP), and also control worms expressing only YFP, in conjunction with fluorescence microscopy

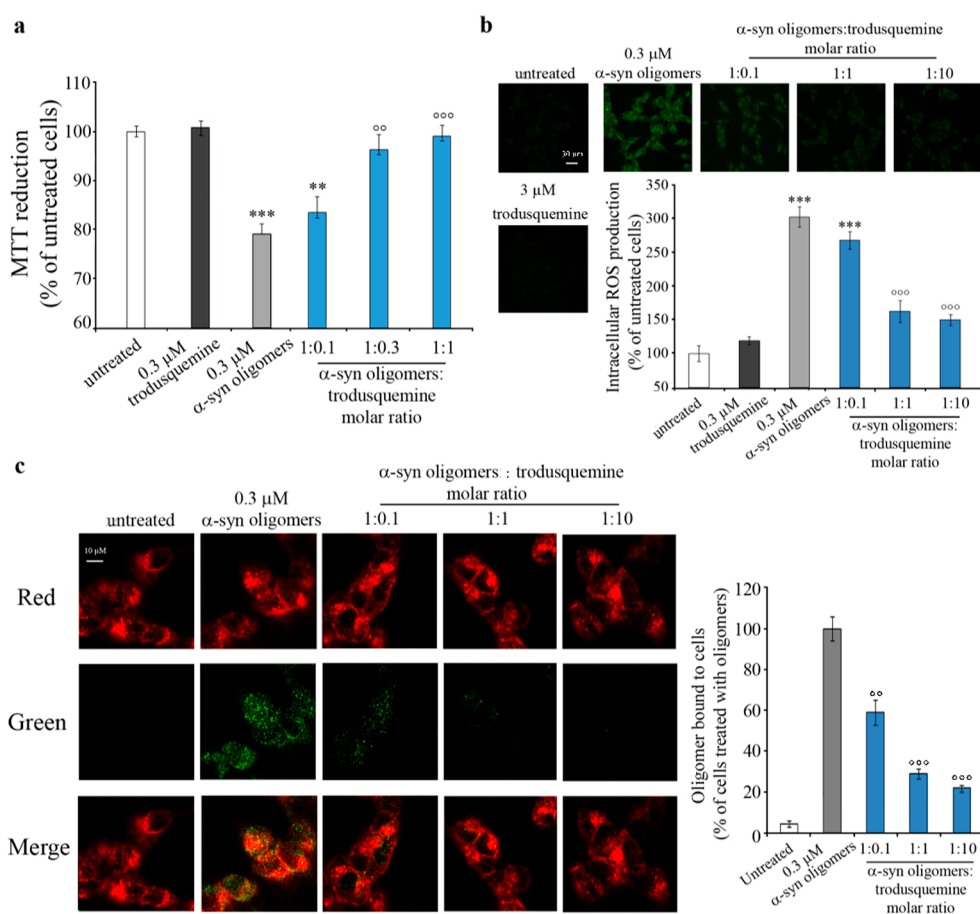


Figure 2. Trodusquemine suppression of the toxicity of α -synuclein oligomers in human neuroblastoma SH-SY5Y cells by inhibition of their binding to cell membranes. (a) Type B* α -synuclein oligomers were resuspended in the cell culture medium at a concentration of 0.3 μ M (monomer equivalents), incubated with or without different concentrations (0.03, 0.1, and 0.3 μ M) of trodusquemine for 1 h at 37 $^{\circ}$ C under shaking conditions and then added to the cell culture medium of SH-SY5Y cells for 24 h to test the ability of the cells to reduce MTT. Experimental errors are SEM *** P \leq 0.001, respectively, relative to untreated cells. °° P \leq 0.01 and °°° P \leq 0.001, respectively, relative to cells treated with α -synuclein oligomers. (b) Top panel: Representative confocal scanning microscope images of SH-SY5Y cells showing the levels of intracellular ROS following a 15 min incubation with 0.3 μ M α -synuclein type B* oligomers (monomer equivalents) in the absence or presence of 0.03, 0.3, and 3.0 μ M trodusquemine. The green fluorescence arises from the CM-H₂DCFDA probe reacting with ROS. Lower panel: quantification. * and ° symbols as in panel A. (c) Representative confocal scanning microscopy images of the apical sections of SH-SY5Y cells treated for 15 min with α -synuclein of type B* oligomers (0.3 μ M monomer equivalents) and different concentrations (0.03, 0.3, or 3.0 μ M) of trodusquemine (left panels). Red and green fluorescence indicate the cell membranes and the α -synuclein oligomers, respectively. Right: quantification of oligomer binding to the cells as a fraction of the cells treated with oligomers (right panel). °° and °°° symbols as in panel A.

328 in order to probe the number and distribution of α -synuclein
 329 inclusions.^{51,52} The expression of YFP in the large muscle cells of
 330 the control animals was uniform and did not lead to the forma-
 331 tion of visible inclusions at D12 of adulthood; furthermore, the
 332 YFP expression pattern was not significantly affected by the adminis-
 333 tration of trodusquemine and was constant with age (Figure 3b).
 334 By contrast, PD worms in the absence of trodusquemine were
 335 found to have large numbers of inclusions at D12, with the
 336 number decreasing significantly (up to 50%) after treatment with
 337 trodusquemine either at the L4 larval stage (p < 0.001 at D12) or
 338 at D5 of adulthood (p < 0.001 at D12). Indeed, treatment of the
 339 PD worms at the L4 larval stage, prior to the appearance of
 340 α -synuclein aggregates, significantly reduced the rate of formation
 341 of visible α -synuclein inclusions as the animals progressed through
 342 adult stages (Figure 3c). In addition, initiation of treatment of the
 343 PD worms as adults on D5, after α -synuclein inclusions had
 344 already appeared in the animals, also significantly decreased the
 345 subsequent rate of formation of inclusions as the animals aged
 346 (Figure 3c).

In an additional series of experiments, the functional behavior
 of the worms was found to be correlated with the observed effects
 on inclusion formation. We observed that PD worms treated at
 the L4 larval stage showed a strongly increased frequency of body
 bends per time unit (p < 0.001 at D14), an increased speed of
 movement (p < 0.001 at D14), and a decreased rate of paralysis
 (p < 0.001 at D14) in comparison to untreated PD worms.
 Indeed, the behavior of the PD worms treated with 10 μ M
 trodusquemine was comparable to that of the healthy control
 worms (Figure 3d). Accordingly, trodusquemine appears to
 share similarities in its mode of action with compounds that
 inhibit the primary nucleation events in protein aggregation such
 as squalamine.²⁹ We observed in addition, however, that PD worms
 treated at D5 of adulthood also showed a greatly decreased fraction
 of paralyzed animals (p < 0.001 at D14) in combination with
 increased body bends per time unit (p < 0.001 at D14) and speed
 of movement (p < 0.001 at D14) (Figure 3d). Taken together,
 these results suggest strongly that trodusquemine has the ability
 to inhibit secondary nucleation as observed *in vitro* (Figure 1).

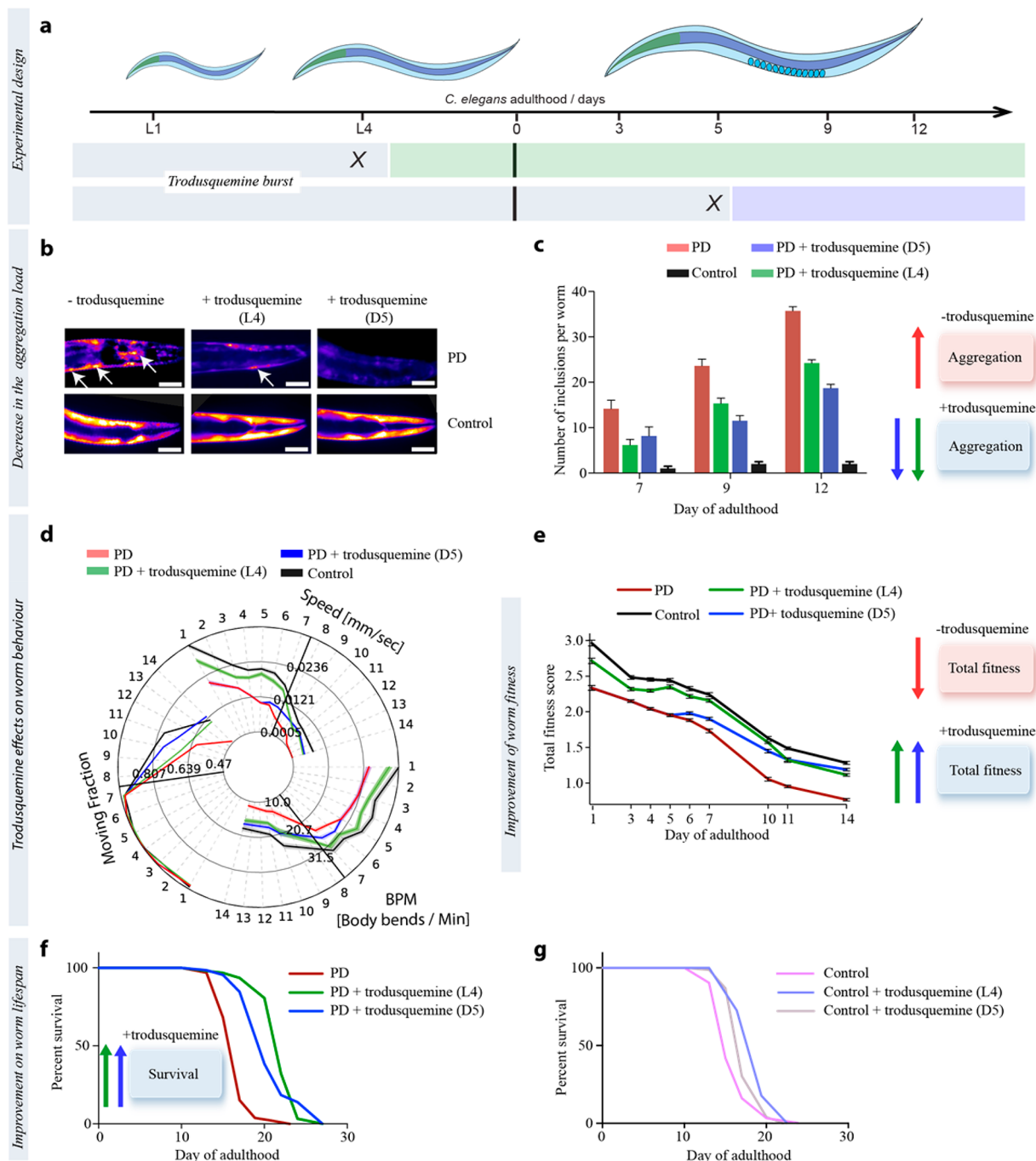


Figure 3. Reduction of the quantity of α -synuclein aggregates and improvement of fitness in *C. elegans* PD model through treatment with trodusquemine. (a) Trodusquemine was administered to the PD worms at either the L4 larval stage or D5 of adulthood. (b) Representative images showing the effects of trodusquemine on PD worms expressing α -synuclein fused to yellow fluorescent protein (YFP). Worms expressing only YFP in the large muscle cells were used as controls. For every experiment, $N = 50$. The images shown are representative of day 12 of adulthood. The scale bar indicates 80 μ m. (c) Effects of trodusquemine on inclusion formation in PD worms at 7, 9, and 12 days of adulthood, respectively. In all panels, the experimental errors refer to SEM. (d) Behavioral map showing the effect of trodusquemine on three phenotypic readouts of worm fitness, i.e. paralysis rate, bends per minute (BPM), and speed of swimming, at the indicated days of adulthood. For every time-point, $N = 500$. (e) Total fitness score quantification,²⁹ following treatment with trodusquemine. For every time-point, $N = 500$. (f,g) Effects following the treatment with trodusquemine on PD (f) and wild type (g) worm survival. For every condition, $N = 75$.

366 Thus, in this animal model of PD, trodusquemine exhibits both
 367 prophylactic and therapeutic efficacy with respect to the forma-
 368 tion of α -synuclein aggregates. By calculating the “total fitness”
 369 score, which is a linear combination of the various types of behav-
 370 ior of the worms, including frequency of body bend, speed of move-
 371 ment, and paralysis rate,²⁹ the significant increase in the health of
 372 PD worms treated with trodusquemine at L4 ($p < 0.001$ at D14)

and D5 ($p < 0.001$ at D14) in comparison to untreated PD 373
 worms is clearly evident (Figure 3e). 374

In addition to such protective actions on the effects of aggre- 375
 gation, exposure of trodusquemine at either L4 ($p < 0.001$ at 376
 D20) or D5 ($p < 0.001$ at D20) significantly increased the longevi- 377
 ty of the PD worms, related to untreated animals (Figure 3f). 378
 The lifespan (described here as the age at which there is the 50% 379

mortality of the population) of untreated PD worms was about 17 ± 1 days, similar to that of control individuals (Figure 3f). Treatment of the PD worms at L4 extended longevity to 24 ± 1 days and at D5 to 20 ± 1 days, in each case exceeding the longevity of healthy control animals. Intriguingly, trodusquemine administration also improved the survival of control animals (Figure 3g), although to a lesser extent, suggesting that the effect of trodusquemine on lifespan is enhanced in the presence of tissue injury caused by the accumulation of α -synuclein inclusions. Longevity in *C. elegans* has been studied extensively, and the roles of multiple pathways including insulin/insulin-like growth factor (IGF)-1 signaling, and dietary restriction, have been shown to influence lifespan.^{53–58} Of particular significance in the context of our observations is the report that trodusquemine can stimulate regeneration in various vertebrate tissues and organs following injury, including those of adult mice, through mobilization of stem cells, with no apparent effect on the growth of uninjured tissues.³⁹ The electrostatic interactions between trodusquemine and membrane-associated phosphatidylinositol 3,4,5-triphosphate (PIP3), driven by the spermine moiety, could also play an important role in this phenomenon, as the displacement of specific PIP3 binding proteins has been shown to increase fitness and longevity in wild type and PD models in *C. elegans*.⁵⁹ Further experiments will, however, be required to define in detail how trodusquemine extends, in particular, the lifespan of the PD worms and its potential relevance to human subjects.

CONCLUSIONS

We have shown that the aminosterol trodusquemine inhibits the lipid-induced initiation of aggregation of α -synuclein *in vitro*, whereas it has no detectable effect on the rate of elongation of fibrils. As with the related aminosterol squalamine, trodusquemine inhibits the initiation of aggregation, but we have also found, however, that it inhibits the secondary nucleation of α -synuclein, thereby reducing the proliferation of the aggregates. The reduction by trodusquemine of both these nucleation processes will reduce substantially the number of potentially toxic aggregates, providing an explanation for the observation of the substantial protective effects of trodusquemine observed both in cultured cells and in a *C. elegans* model of PD. As with squalamine,²⁹ trodusquemine appears to be able to displace α -synuclein and its oligomers from the membrane, inhibiting both the lipid-induced initiation of the aggregation process and the ability of the oligomers to disrupt the integrity of membranes. In addition, these molecules may interact directly with the oligomers to reduce their inherent toxicity. Intriguingly, administration of trodusquemine also extends the longevity of the PD worms, beyond even that of control animals and to an extent larger than that observed with squalamine. Taken together, these results suggest that trodusquemine, which can cross the blood–brain barrier, could have multiple benefits in the context of human α -synucleinopathies, ranging from an increased understanding of the nature and progression of these conditions to disease modification and tissue regeneration.

MATERIALS AND METHODS

Reagents. 1,2-Dimyristoyl-*sn*-glycero-3-phospho-L-serine (sodium salt; DMPS) was purchased from Avanti Polar Lipids (Alabaster, AL, USA). Trodusquemine (as the chloride salt) was synthesized as previously described³¹ and was greater than 97% pure as evaluated by mass spectrometry. Trodusquemine powder was used immediately after dilution.

Protein Expression and Lipid Preparation. Wild type human α -synuclein was recombinantly expressed and purified as described previously.^{14,15} For concentration measurements, we used an extinction coefficient of 5600 M⁻¹ cm⁻¹ at 275 nm. After the final size-exclusion chromatography step (20 mM phosphate buffer, pH 6.5), the protein was snap frozen in liquid nitrogen in the form of 1 mL aliquots and stored at -80 °C. These aliquots were used without further treatment, except for the aggregation experiments at low pH where the pH was adjusted to the desired value with small volumes of 100 mM NaOH or HCl. The lipids were dissolved in 20 mM phosphate buffer (NaH₂PO₄/Na₂HPO₄), pH 6.5, and 0.01% NaN₃ and stirred at ca. 45 °C for 2 h. The solution was then frozen and thawed five times using dry ice and a water bath at 45 °C. The preparation of vesicles was carried out on ice by means of sonication (3 × 5 min, 50% cycles, 10% maximum power on ice) using a Bandelin Sonopuls HD 2070 (Bandelin, Berlin, Germany). After centrifugation, the sizes of the vesicles were checked using dynamic light scattering (Zetasizer Nano ZSP, Malvern Instruments, Malvern, UK) and were shown to consist of a distribution centered on a diameter of 20 nm.

Circular Dichroism (CD) Spectroscopy. Data Acquisition. Samples were prepared as described previously²⁹ by incubating 5 μ M α -synuclein with 250 μ M DMPS vesicles in 20 mM phosphate buffer, pH 6.5, 0.01% NaN₃, and 0–50 μ M trodusquemine. Far-UV CD spectra were recorded on a JASCO J-810 instrument (Tokyo, Japan) equipped with a Peltier thermally controlled cuvette holder at 30 °C. Quartz cuvettes with path lengths of 1 mm were used, and the CD signal was measured in each case at 222 nm by averaging 60 individual measurements with a bandwidth of 1 nm, a data pitch of 0.2 nm, a scanning speed of 50 nm/min, and a response time of 1 s. The signal of the buffer containing DMPS and the different concentrations of trodusquemine was subtracted from that of the protein.

Data Analysis. The concentration of α -synuclein bound to DMPS vesicles ($[\alpha_b]$) when 5 μ M α -synuclein was incubated in the presence of 250 μ M DMPS and increasing concentrations of trodusquemine ($[T]$) was calculated from the CD signal measured at 222 nm as described previously.¹⁴ The change in $[\alpha_b]$ with increasing $[T]$ was then analyzed as described previously²⁹ using the standard solution of the cubic equation:

$$K_{D,\alpha} = \frac{([\text{DMPS}] - L_T[T_b] - L_\alpha[\alpha_b])([\alpha] - [\alpha_b])}{L_\alpha[\alpha_b]} \quad (1)$$

$$[T_b] = \left([\text{DMPS}] - L_\alpha[\alpha_b] + K_{D,T}L_T + L_T[T] - (4L_T([\alpha_b]L_\alpha[T] - [\text{DMPS}][T]) + ([\text{DMPS}] - [\alpha_b]L_\alpha + K_{D,T}L_T + L_T[T])^2)^{-1/2} \right) / (2L_T) \quad (2)$$

where $K_{D,\alpha}$ and $K_{D,T}$ are the binding constants of α -synuclein and trodusquemine, respectively; L_α and L_T are the stoichiometries at which DMPS binds to α -synuclein and trodusquemine, i.e., the number of lipid molecules interacting with one molecule of either α -synuclein or trodusquemine, respectively; $[\text{DMPS}]$, $[\alpha]$, and $[T]$ are the total concentrations of DMPS, α -synuclein, and trodusquemine, respectively; and $[\alpha_b]$ and $[T_b]$ are the concentrations of α -synuclein and trodusquemine bound to DMPS vesicles, respectively. The best fit is shown in Figure S2 with $K_{D,T} = 1.62 \times 10^{-8}$ M and $[L_T] = 5.1$. For further details of the analysis, see the Supporting Information.

Dynamic Light Scattering (DLS) Measurements. Measurements of vesicle size distributions in the absence and presence of the indicated concentrations of trodusquemine were carried out by dynamic light scattering (DLS) experiments using a Zetasizer Nano ZSP Instrument (Malvern Instruments, Malvern, UK) with backscatter detection at a scattering angle of 173°. The concentration of the vesicles was 0.1 mM

497 in phosphate buffer (20 mM, pH 6.5) and the experiments were carried
498 out at a temperature of 25 °C.

499 **Aggregation Kinetics in the Presence of Lipid Vesicles.** *Data*
500 *Acquisition.* α -Synuclein was incubated at a concentration of 20–100 μM
501 in 20 mM sodium phosphate, pH 6.5, and 0.01% NaN_3 , in the presence
502 of 50 μM ThT, 100 μM DMPS vesicles, and increasing concentrations of
503 trodusquemin (0 to 10 μM).²⁹ The stock solution of trodusquemin
504 was prepared by dissolving the molecule in 20 mM phosphate buffer to a
505 final concentration of 100 μM . The change in the ThT fluorescence
506 signal with time was monitored using a Fluostar Optima or a Polarstar
507 Omega (BMG Labtech, Aylesbury, UK) fluorimeter under quiescent
508 conditions at 30 °C.²⁹ Corning 96-well plates with half-area (black/clear
509 bottom) nonbinding surfaces (Sigma-Aldrich, St. Louis, MO, USA)
510 were used for each experiment.

511 *Data Analysis.* The early times of the aggregation curves of
512 α -synuclein in the presence of DMPS and different concentrations of
513 trodusquemin were fitted using the one-step nucleation model
514 described previously¹⁴ and the following equation:

$$M(t) = \frac{K_M k_n m(0)^{n+1} k_+ [\text{DMPS}] t^2}{2(K_M + m(0)) L_\alpha} \quad (3)$$

516 where t is the time, $M(t)$ is the aggregate mass, $m(0)$ is the free monomer
517 concentration, K_M is the saturation constant of the elongation process
518 (125 μM),¹⁴ k_n and k_+ are the rate constants of nucleation and elonga-
519 tion, respectively, and $[\text{DMPS}]/L_\alpha$ is the concentration of protein-
520 binding sites at the surface of the membrane. First, the early times of the
521 kinetic traces measured for α -synuclein in the presence of 100 μM
522 DMPS and in the absence of trodusquemin were fitted using eq 3, with
523 k_n, k_+ and n being global fitting parameters (see fits in Figure S4a).
524 The global fit yields $n = 0.745$ and $k_n k_+ = 8.6 \times 10^{-3} \text{ M}^{-(n+1)} \cdot \text{s}^{-2}$. We then
525 fixed n to 0.745 and fitted the early times of the data in the presence of
526 trodusquemin using eq 3, with k_n, k_+ being the only global fitting param-
527 eter (see Figure S4b–f). This way, we obtain the effective rate of lipid-
528 induced aggregation of α -synuclein relative to that in the absence of
529 trodusquemin, at all α -synuclein and trodusquemin concentrations
530 (see Figure S5):

$$r_{\text{eff}} = \frac{k_n k_+}{k_n k_+} \quad (4)$$

532 where $k_n k_+$ is the product of the nucleation and elongation rate constants
533 at a given [trodusquemin]/[α -synuclein] ratio. If trodusquemin were
534 to inhibit α -synuclein lipid-induced aggregation *via* the same mechanism
535 as that reported previously for squalamine²⁹ and β -synuclein,^{14,41} the
536 effective rate should scale with a power of the coverage, i.e., $r_{\text{eff}} = \theta_\alpha^{n_b}$,
537 where θ_α is the fractional coverage of a lipid vesicle in α -synuclein and n_b
538 is the reaction order of lipid-induced aggregation with respect to θ_α .
539 In the absence of trodusquemin, $\theta_\alpha = 1$, as we are in a regime where the
540 vesicles are saturated. We determined θ_α for the different [trodusque-
541 mine]/[α -synuclein] ratios used in our study using a simplified com-
542 petitive binding model with the values of $K_{D,T}$ and L_T determined in this
543 study and $K_{D,\alpha}$ and L_α determined previously,¹⁴ using $n_b = 5.5$, as deter-
544 mined previously,^{29,41} and the following equations:

$$\theta_\alpha = \frac{[\alpha_b] L_\alpha}{[\text{DMPS}]} \quad (5)$$

$$[\alpha_b] = \frac{([\text{DMPS}] L_\alpha \kappa - [\text{DMPS}] L_T - [\alpha] L_\alpha L_T - L_\alpha L_T [\text{T}] \kappa)}{(2(L_\alpha^2 \kappa - L_\alpha L_T)) + ((4[\alpha][\text{DMPS}] L_T (L_\alpha^2 \kappa - L_\alpha L_T) + ([\text{DMPS}] L_T + [\alpha] L_\alpha L_T - [\text{DMPS}] L_\alpha \kappa + L_\alpha L_T [\text{T}] \kappa)^2)^{-1/2}} / (2(L_\alpha^2 \kappa - L_\alpha L_T)) \quad (6)$$

547 where $\kappa = K_{D,\alpha}/K_{D,T}$.

548 We found that the values of r_{eff} obtained at different [trodusque-
549 mine]/[α -synuclein] ratios do not scale simply as $\theta_\alpha^{n_b}$, with the coverage
550 θ_α calculated using eqs 5 and 6 at the corresponding ratios, suggesting
551 that trodusquemin inhibits α -synuclein lipid-induced aggregation *via*
552 a more complex mechanism than that described for squalamine

(see Figure S5), perhaps resulting from a direct interaction with the
553 oligomeric species resulting in an inhibition of their inherent toxicity.

554 **Seed Fibril Formation.** Seed fibrils were produced as previously
555 described.^{15,41} Briefly, we incubated 500 μL solutions of α -synuclein at
556 concentrations between 500 and 800 μM in 20 mM phosphate buffer at
557 pH 6.5 for 48–72 h at ca. 40 °C with maximal stirring with a Teflon bar
558 on an RCT Basic Heat Plate (IKA, Staufen, Germany). The fibrils were
559 divided into aliquots, frozen in liquid N_2 , and stored at -80 °C until
560 required. For aggregation experiments, the seed fibrils were diluted to
561 200 μM monomer equivalents into the specific buffer to be used in the
562 experiment and sonicated three times for 10 s using a Bandelin Sonopuls
563 HD 2070 probe sonicator (Bandelin, Berlin, Germany), using 10% maxi-
564 mum power and 30% cycles.

565 **Seeded Aggregation Kinetics.** The seeded experiments were per-
566 formed as described previously.^{15,41} Briefly, to probe fibril elongation,
567 preformed seed fibrils (5 μM monomer equivalents) were added to
568 solutions of monomeric α -synuclein (20–100 μM) in 20 mM phosphate
569 buffer (pH 6.5) with 50 μM ThT, under quiescent conditions, at 37 °C.
570 For experiments to probe the influence on secondary nucleation, seeds
571 (50 nM monomer equivalents) were added to monomeric α -synuclein
572 (60–100 μM) in 20 mM phosphate buffer (pH 4.8) and in the presence
573 of 50 μM ThT, under quiescent conditions, also at 37 °C. The increase
574 in ThT fluorescence was monitored in low binding, clear-bottomed half-
575 area Corning 96 well plates (Sigma-Aldrich, St. Louis, MO, USA) that
576 were sealed with tape, and using either a Fluostar Optima, Polarstar
577 Omega (BMG Labtech, Aylesbury, UK), or M1000 (Tecan Group Ltd.,
578 Männedorf, Switzerland) fluorescence plate-reader in bottom reading
579 mode. All experiments were performed under quiescent conditions
580 (i.e., without shaking).

581 **Data Analysis.** Data were analyzed as previously described.^{15,41}

582 **Mass Spectrometry.** Experiments were carried out as previously
583 described.²⁹ Briefly, fibrils of α -synuclein at a concentration of 10 μM
584 (monomer equivalents) were incubated with 10 μM trodusquemin in
585 20 mM Tris, pH 7.4, and 100 mM NaCl overnight under quiescent
586 conditions at RT. The samples were then centrifuged at 100,000g for
587 30 min and the supernatant then removed for analysis. Samples for the
588 analysis by mass spectrometry were prepared as described,²⁹ and the
589 experiments were run using a Waters Xevo G2-S QTOF spectrometer
590 (Waters Corporation, MA, USA).

591 **Nuclear Magnetic Resonance (NMR) Spectroscopy.** H_2O was
592 removed from trodusquemin by three cycles of lyophilization, and the
593 compound was resoluted in 100% D_2O (Sigma-Aldrich). It was then
594 diluted into 20 mM phosphate buffer, pH 6.5, in 100% D_2O to a final
595 concentration of 10 μM . All NMR measurements were performed at
596 30 °C on a Bruker AVANCE-500 spectrometer, operated at a ^1H fre-
597 quency of 500.13 MHz, equipped with a cryogenic probe. Measure-
598 ments of diffusion coefficients were performed using 2D ^1H diffusion
599 ordered spectroscopy (DOSY) experiments.⁶⁰ These spectra were
600 acquired using the standard “*ledbpgppr2s*” Bruker pulse program, using a
601 bipolar gradient pulse pair-stimulated echo sequence incorporating a
602 longitudinal eddy current delay,⁶¹ with a diffusion time (Δ) of 100 ms
603 and a gradient pulse length (δ) of 3 ms and increasing the gradient
604 strength between $4.8 < g < 38.5 \text{ G cm}^{-1}$. The values of Δ and δ were
605 chosen based on measurements of 1.5 mM trodusquemin in water, in
606 which it is very soluble. To remove the signal from residual H_2O in the
607 sample, presaturation was used. Data for 1.5 mM trodusquemin in
608 100% D_2O were collected with eight scans and 16 gradient steps, while
609 data for 10 μM trodusquemin in 20 mM phosphate buffer were
610 collected with 400 scans and 12 gradient steps. Individual rows of the
611 pseudo-2D diffusion data were phased and baseline corrected. DOSY
612 spectra were processed using the TopSpin 2.1 software (Bruker). The
613 diffusion dimension was generated using the intensities (I) of resolved
614 peaks between 3.0 and -0.5 ppm according to the Stejskal–Tanner
615 equation⁶²

$$\frac{I}{I_0} = e^{-\gamma^2 g^2 \delta^2 D (\Delta - \frac{\delta}{3})}$$

617 where γ is the gyromagnetic ratio, and using the DynamicsCenter
618 2.5.3 software (Bruker). 1D ^1H NMR spectra of 10 μM trodusquemin

alone in 20 mM phosphate buffer, pH 6.5 and 30 °C, made up in 100% D₂O or in the presence of equimolar 4,4-dimethyl-4-silapentane-1-sulfonic acid (DSS, Sigma-Aldrich) as an internal concentration standard. These spectra were acquired using the standard “noesypr1d” Bruker pulse program with presaturation to remove the signal from residual H₂O in the sample. Spectra were processed using TopSpin 2.1.

ThT Binding to Trodusquemine. Preformed fibrils of α -synuclein (5 μ M) were added to monomeric α -synuclein at a concentration of 100 μ M and incubated in 96-well half-area, low-binding polyethylene glycol coating plate (Corning 3881, Kennebuck ME, USA) at 37 °C in 20 mM phosphate buffer (pH 6.5) under quiescent conditions for 24 h. Then, the resulting longer fibrils were diluted to 50 μ M α -synuclein with 50 μ M ThT and the absence or presence of the indicated concentration of trodusquemine in 20 mM phosphate buffer (pH 6.5) and incubated at 37 °C for 12 h. The fluorescence intensity of the different samples was measured using a plate reader (Fluostar Optima, BMG Labtech, Ortenberg, Germany).

Preparation of Oligomers. Samples of α -synuclein type B* oligomers were prepared as previously described.⁴⁷ Briefly, monomeric α -synuclein was lyophilized in Milli-Q water and subsequently resuspended in PBS, pH 7.4, to give a final concentration of ca. 800 μ M (12 mg mL⁻¹). The resulting solutions were passed through a 0.22 μ m cutoff filter before incubation at 37 °C for 20–24 h under quiescent conditions.⁴⁷ Very small amounts of fibrillar species formed during this time were removed by ultracentrifugation for 1 h at 90 000 rpm (using a TLA-120.2 Beckman rotor, 288 000g). Excess monomeric protein and any small oligomeric species were then removed by multiple cycles of filtration using 100 kDa cutoff membranes. The final concentration of the prepared oligomers was estimated using $\epsilon_{275} = 5600 \text{ M}^{-1} \text{ cm}^{-1}$.

Neuroblastoma Cell Cultures. Human SH-SY5Y neuroblastoma cells (A.T.C.C., Manassas, VA, USA) were cultured in DMEM, F-12 HAM with 25 mM HEPES, and NaHCO₃ (1:1) and supplemented with 10% FBS, 1 mM glutamine, and 1.0% antibiotics. Cell cultures were maintained in a 5% CO₂ humidified atmosphere at 37 °C and grown until they reached 80% confluence for a maximum of 20 passages.⁶³

MTT Reduction Assay. α -Synuclein oligomers (0.3 μ M monomer equivalents) were incubated without or with increasing concentrations (0.03, 0.1, and 0.3) of trodusquemine for 1 h at 37 °C under shaking conditions and then added to the cell culture medium of SH-SY5Y cells seeded in 96-well plates for 24 h. The 3-(4,5-dimethylthiazol-2-yl)-2,5-diphenyltetrazolium bromide (MTT) reduction assay was performed as previously described.⁶⁴

Measurement of Intracellular ROS. SH-SY5Y cells were seeded on glass coverslips and treated for 15 min with α -synuclein oligomers (0.3 μ M) and increasing concentrations (0.03, 0.3, and 3 μ M) of trodusquemine. After incubation, the cells were washed with PBS and loaded with 10 μ M 2',7'-dichlorodihydrofluorescein diacetate (CM-H₂DCFDA; Life Technologies, CA, USA) as previously described.⁶³ The fluorescence of the cells was then analyzed by means of a TCS SP5 scanning confocal microscopy system (Leica Microsystems, Mannheim, Germany) equipped with an argon laser source, using the 488 nm excitation line. A series of 1.0- μ m-thick optical sections (1024 × 1024 pixels) was taken through the cells for each sample using a Leica Plan Apo 63 oil immersion objective.

Oligomer Binding to Cellular Membranes. SH-SY5Y cells were seeded on glass coverslips and treated for 15 min with α -synuclein oligomers (0.3 μ M) and increasing concentrations (0.03, 0.3, and 3 μ M) of trodusquemine. After incubation, the cells were washed with PBS and counterstained with 5.0 μ g/mL Alexa Fluor 633-conjugated wheat germ agglutinin (Life Technologies, CA, USA) to label fluorescently the cellular membrane.²⁹ After washing with PBS, the cells were fixed in 2% (w/v) buffered paraformaldehyde for 10 min at RT (20 °C). The presence of oligomers was detected with 1:250 diluted rabbit polyclonal anti- α -synuclein antibodies (Abcam, Cambridge, UK) and subsequently with 1:1000 diluted Alexa Fluor 488-conjugated anti-rabbit secondary antibodies (Life Technologies, CA, USA). Fluorescence emission was detected after double excitation at 488 and 633 nm by the scanning confocal microscopy system described above,

and three apical sections were projected as a single composite image by superimposition.

C. elegans Media. Standard conditions were used for the propagation of *C. elegans*.⁶⁵ Briefly, the animals were synchronized by hypochlorite bleaching, hatched overnight in M9 (3 g/L KH₂PO₄, 6 g/L Na₂HPO₄, 5 g/L NaCl, 1 μ M MgSO₄) buffer, and subsequently cultured at 20 °C on nematode growth medium (NGM) plates (1 mM CaCl₂, 1 mM MgSO₄, 5 μ g/mL cholesterol, 250 μ M KH₂PO₄, pH 6, 17 g/L Agar, 3g/L NaCl, 7.5 g/L casein) seeded with the *E. coli* strain OP50. Saturated cultures of OP50 were grown by inoculating 50 mL of LB medium (10 g/L tryptone, 10 g/L NaCl, 5 g/L yeast extract) with OP50 cells and incubating the culture for 16 h at 37 °C. NGM plates were seeded with bacteria by adding 350 μ L of saturated OP50 cells to each plate and leaving the plates at 20 °C for 2–3 days. On day 3 after synchronization, the animals were placed on NGM plates containing 75 μ M 5-fluoro-2'-deoxyuridine (FUDR).

Strains. The following strains were used: zgIs15 [P(unc-54):: α -syn::YFP]IV (OW40), in which α -synuclein fused to YFP relocates to inclusions, which are visible as early as day 2 after hatching and increase in number and size during the aging of the animals, up to late adulthood (day 17),^{29,66} and rmIs126 [P(unc-54)Q0::YFP]V (OW450). In OW450, YFP alone is expressed and remains diffusely localized throughout aging.^{29,66}

Trodusquemine-coated plates. Plates were prepared as previously described.²⁹ Briefly, aliquots of NGM media were autoclaved, poured, and seeded with 350 μ L of OP50 culture and grown overnight at RT. After incubating for up to 3 days at RT, aliquots of trodusquemine dissolved in water at different concentrations were added. NGM plates containing FUDR (75 μ M, unless stated otherwise) were seeded with aliquots of the trodusquemine dissolved in water, at the appropriate concentration. The plates were then placed in a laminar flow hood at RT to dry, and the worms were transferred to plates coated with trodusquemine at larval stage L4.

Automated Motility Assay. All *C. elegans* populations were cultured at 20 °C and developmentally synchronized from a 4 h egg-lay. At 64–72 h post-egg-lay (time zero), individuals were transferred to FUDR plates, and body movements were assessed over the times indicated. At different ages, the animals were washed off the plates with M9 buffer and spread over an OP-50 unseeded 6 cm plate, after which their movements were recorded at 30 fps using a recently developed microscopic procedure for 30 s or 1 min.²⁹ Up to 200 animals were counted in each experiment unless otherwise stated. One experiment that is representative of the three measured in each series of experiments is shown, and videos were analyzed using a custom-made tracking code.^{29,67}

Lifespan Assays. Lifespan analysis was carried out as previously described.⁶⁸ On day 4 after synchronization, the animals were placed on NGM plates containing FUDR. On L4 or D5, they were manually transferred to plates seeded with 10 μ M trodusquemine. Experiments were performed at 20 °C. Lifespan experiments were performed with 75 animals per condition. At each time point, the number of surviving animals, determined by movement and response to nose touch, was counted. Animals that crawled out of the plates during the assay were excluded. Three independent experiments were carried out in each case, and one representative is shown. Analysis was performed using GraphPad Prism (GraphPad Software).

Quantification of Inclusions. Individual animals were mounted on 2% agarose pads, containing 40 mM NaN₃ as an anesthetic, on glass microscope slides for imaging.²⁹ Only the frontal region of the worms was considered.^{29,66} The numbers of inclusions in each animal were quantified using a Leica MZ16 FA fluorescence dissection stereomicroscope (Leica Microsystems, Wetzlar, Germany) at a nominal magnification of 20 \times or 40 \times , and images were acquired using an Evolve 512 Delta EMCCD Camera, with high quantum efficiency (Photometrics, Tucson, AZ, USA). Measurements on inclusions were performed using ImageJ software.²⁹ All experiments were carried out in triplicate, and the data from one representative experiment are shown in the figure. The Student's *t* test was used to calculate *p* values, and all tests were two-tailed unpaired unless otherwise stated. At least 50 animals were examined per condition, unless stated otherwise.

759 ■ ASSOCIATED CONTENT

760 ■ Supporting Information

761 The Supporting Information is available free of charge on the ACS
762 Publications website at DOI: 10.1021/acschembio.8b00466.

763 Experimental procedures and characterization including
764 the structure of trodusquemine and sequence of α -synuclein,
765 dynamic light scattering (DLS), circular dichroism (CD),
766 lipid induced aggregation, global analysis of kinetic traces,
767 effective rate of α -synuclein lipid-induced aggregation,
768 fibril elongation and relative rates, fibril amplification and
769 relative rates, mass spectrometry, ThT binding, nuclear
770 magnetic resonance (NMR) (DOCX)

771 ■ AUTHOR INFORMATION

772 Corresponding Authors

773 *E-mail: fabrizio.chiti@unifi.it.

774 *E-mail: maz5@georgetown.edu.

775 *E-mail: mv245@cam.ac.uk.

776 *E-mail: cmd44@cam.ac.uk.

777 ORCID 

778 Michele Perni: 0000-0001-7593-8376

779 Patrick Flagmeier: 0000-0002-1204-5340

780 Francesco A. Aprile: 0000-0002-5040-4420

781 Céline Galvagnion: 0000-0001-9753-3310

782 Gabriella T. Heller: 0000-0002-5672-0467

783 Georg Meisl: 0000-0002-6562-7715

784 Janet R. Kumita: 0000-0002-3887-4964

785 Pavan K. Challa: 0000-0002-0863-381X

786 Tuomas P. J. Knowles: 0000-0002-7879-0140

787 Fabrizio Chiti: 0000-0002-1330-1289

788 Michele Vendruscolo: 0000-0002-3616-1610

789 Author Contributions

790 [†]These authors made equal contributions

791 Author Contributions

792 M.P., P.F., R.L., F.A., C.G., T.P.J.K., D.B., M.Z., M.V., F.C., C.C.,
793 and C.M.D. were involved in the design of the study. M.P. and
794 R.L. performed the *C. elegans* experiments. P.F. and C.G. carried
795 out the *in vitro* experiments. P.F., C.G., and G.M. analyzed the
796 kinetic data of α -synuclein aggregation. R.C. carried out the cell
797 experiments. G.T.H. performed the NMR experiments. S.W.C.
798 purified the α -synuclein oligomers. M.P., P.F., R.L., M.Z., M.V.,
799 F.C., and C.M.D. wrote the paper, and all the authors were
800 involved in the analysis of the data and editing of the paper.

801 Notes

802 The authors declare the following competing financial
803 interest(s): M.Z. and D.B. own patents for the use of
804 Trodusquemine in the treatment of Parkinson's disease.

805 ■ ACKNOWLEDGMENTS

806 This work was supported by the Boehringer Ingelheim Fonds
807 (P.F.), the Studienstiftung des Deutschen Volkes (P.F.), Gates
808 Cambridge Scholarships (R.L. and G.T.H.) and a St. John's
809 College Benefactors' Scholarship (R.L.), the UK Biotechnology
810 and Biochemical Sciences Research Council (M.V. and C.M.D.),
811 a Senior Research Fellowship award from the Alzheimer's
812 Society, UK, (F.A.A.), the Wellcome Trust (C.M.D., M.V., and
813 T.P.J.K.), the Frances and Augustus Newman Foundation
814 (T.P.J.K.), the Regione Toscana—FAS Salute—Supremal
815 project (R.C., C.C., and F.C.), a Marie Skłodowska-Curie
816 Actions—Individual Fellowship (C.G.), Sidney Sussex College

Cambridge (G.M.), the Spanish Government—MINECO 817
(N.C.), and by the Cambridge Centre for Misfolding Diseases 818
(M.P., P.F., R.L., F.A.A., C.G., G.T.H., S.W.C., J.R.K., T.P.J.K., 819
M.V., and C.M.D.). The authors would like to thank E. Klimont 820
for her assistance with the expression and purification of 821
 α -synuclein and N. Fernando for assistance with the *C. elegans* 822
experiments. We acknowledge the NMR Service at the 823
Chemistry Department of the University of Cambridge for 824
helpful discussions, particularly P. Grice and D. Howe and the 825
UK EPSRC for Core Capabilities funding (EP/K039520/1). 826

■ REFERENCES 827

- (1) Bodner, C. R., Dobson, C. M., and Bax, A. (2009) Multiple tight 828
phospholipid-binding modes of alpha-synuclein revealed by solution 829
NMR spectroscopy. *J. Mol. Biol.* 390, 775–790. 830
- (2) Wilhelm, B. G., Mandad, S., Truckenbrodt, S., et al. (2014) 831
Composition of isolated synaptic boutons reveals the amounts of vesicle 832
trafficking proteins. *Science* 344, 1023–1028. 833
- (3) Maroteaux, L., Campanelli, J. T., and Scheller, R. H. (1988) 834
Synuclein: a neuron-specific protein localized to the nucleus and 835
presynaptic nerve terminal. *J. Neurosci.* 8, 2804–2815. 836
- (4) Takeda, A., Mallory, M., Sundsmo, M., Honer, W., Hansen, L., and 837
Masliah, E. (1998) Abnormal accumulation of NACP/alpha-synuclein 838
in neurodegenerative disorders. *Am. J. Pathol.* 152, 367–372. 839
- (5) Spillantini, M. G., Crowther, R. A., Jakes, R., Hasegawa, M., and 840
Goedert, M. (1998) alpha-Synuclein in filamentous inclusions of Lewy 841
bodies from Parkinson's disease and dementia with lewy bodies. *Proc.* 842
Natl. Acad. Sci. U. S. A. 95, 6469–6473. 843
- (6) Dettmer, U., Selkoe, D., and Bartels, T. (2016) New insights into 844
cellular α -synuclein homeostasis in health and disease. *Curr. Opin.* 845
Neurobiol. 36, 15–22. 846
- (7) Dawson, T. M., and Dawson, V. L. (2003) Molecular pathways of 847
neurodegeneration in Parkinson's disease. *Science* 302, 819–822. 848
- (8) Knowles, T. P. J., Vendruscolo, M., and Dobson, C. M. (2014) The 849
amyloid state and its association with protein misfolding diseases. *Nat.* 850
Rev. Mol. Cell Biol. 15, 384–396. 851
- (9) Chiti, F., and Dobson, C. M. (2006) Protein misfolding, functional 852
amyloid, and human disease. *Annu. Rev. Biochem.* 75, 333–366. 853
- (10) Lee, V. M. Y., and Trojanowski, J. Q. (2006) Mechanisms of 854
Parkinson's disease linked to pathological alpha-synuclein: new targets 855
for drug discovery. *Neuron* 52, 33–38. 856
- (11) Tong, J., Wong, H., Guttman, M., Ang, L. C., Forno, L. S., 857
Shimadzu, M., Rajput, A. H., Muentner, M. D., Kish, S. J., Hornykiewicz, 858
O., and Furukawa, Y. (2010) Brain α -synuclein accumulation in multiple 859
system atrophy, Parkinson's disease and progressive supranuclear palsy: 860
a comparative investigation. *Brain* 133, 172–188. 861
- (12) Chiti, F., and Dobson, C. M. (2017) Protein misfolding, amyloid 862
formation, and human disease: a summary of progress over the last 863
decade. *Annu. Rev. Biochem.* 86, 27–68. 864
- (13) Buell, A. K., Galvagnion, C., Gaspar, R., Sparr, E., Vendruscolo, 865
M., Knowles, T. P. J., Linse, S., and Dobson, C. M. (2014) Solution 866
conditions determine the relative importance of nucleation and growth 867
processes in α -synuclein aggregation. *Proc. Natl. Acad. Sci. U. S. A.* 111, 868
7671–7676. 869
- (14) Galvagnion, C., Buell, A. K., Meisl, G., Michaels, T. C. T., 870
Vendruscolo, M., Knowles, T. P. J., and Dobson, C. M. (2015) Lipid 871
vesicles trigger α -synuclein aggregation by stimulating primary 872
nucleation. *Nat. Chem. Biol.* 11, 229–234. 873
- (15) Flagmeier, P., Meisl, G., Vendruscolo, M., Knowles, T. P. J., 874
Dobson, C. M., Buell, A. K., and Galvagnion, C. (2016) Mutations 875
associated with familial Parkinson's disease alter the initiation and 876
amplification steps of α -synuclein aggregation. *Proc. Natl. Acad. Sci. U. S.* 877
A. 113, 10328–10333. 878
- (16) Fink, A. L. (2006) The aggregation and fibrillation of alpha- 879
synuclein. *Acc. Chem. Res.* 39, 628–634. 880
- (17) Munishkina, L. A., Phelan, C., Uversky, V. N., and Fink, A. L. 881
(2003) Conformational behavior and aggregation of alpha-synuclein in 882

- 883 organic solvents: modeling the effects of membranes. *Biochemistry* 42,
884 2720–2730.
- 885 (18) Munishkina, L. A., Henriques, J., Uversky, V. N., and Fink, A. L.
886 (2004) Role of protein-water interactions and electrostatics in alpha-
887 synuclein fibril formation. *Biochemistry* 43, 3289–3300.
- 888 (19) Uversky, V. N., Li, J., Souillac, P., Millett, I. S., Doniach, S., Jakes,
889 R., Goedert, M., and Fink, A. L. (2002) Biophysical properties of the
890 synucleins and their propensities to fibrillate: inhibition of alpha-
891 synuclein assembly by beta- and gamma-synucleins. *J. Biol. Chem.* 277,
892 11970–11978.
- 893 (20) Uversky, V. N., Li, J., and Fink, A. L. (2001) Evidence for a
894 partially folded intermediate in alpha-synuclein fibril formation. *J. Biol.*
895 *Chem.* 276, 10737–10744.
- 896 (21) Heise, H., Hoyer, W., Becker, S., Andronesi, O. C., Riedel, D., and
897 Baldus, M. (2005) Molecular-level secondary structure, polymorphism,
898 and dynamics of full-length α -synuclein fibrils studied by solid-state
899 NMR. *Proc. Natl. Acad. Sci. U. S. A.* 102 (44), 15871–6.
- 900 (22) Vilar, M., Chou, H.-T., Lühns, T., Maji, S. K., Riek-Loher, D.,
901 Verel, R., Manning, G., Stahlberg, H., and Riek, R. (2008) The fold of
902 alpha-synuclein fibrils. *Proc. Natl. Acad. Sci. U. S. A.* 105, 8637–8642.
- 903 (23) Comellas, G., Lemkau, L. R., Nieuwkoop, A. J., Klopper, K. D.,
904 Lador, D. T., Ebisu, R., Woods, W. S., Lipton, A. S., George, J. M., and
905 Rienstra, C. M. (2011) Structured regions of α -synuclein fibrils include
906 the early-onset Parkinson's disease mutation sites. *J. Mol. Biol.* 411, 881–
907 895.
- 908 (24) Gath, J., Bousset, L., Habenstein, B., Melki, R., Böckmann, A., and
909 Meier, B. H. (2014) Unlike twins: an NMR comparison of two α -
910 synuclein polymorphs featuring different toxicity. *PLoS One* 9, e90659–
911 90659.
- 912 (25) Gath, J., Bousset, L., Habenstein, B., Melki, R., Meier, B. H., and
913 Böckmann, A. (2014) Yet another polymorph of α -synuclein: solid-state
914 sequential assignments. *Biomol. NMR Assignments* 8, 395–404.
- 915 (26) Tuttle, M. D., Comellas, G., Nieuwkoop, A. J., Covell, D. J.,
916 Berthold, D. A., Klopper, K. D., Courtney, J. M., Kim, J. K., Barclay, A.
917 M., Kendall, A., Wan, W., Stubbs, G., Schwieters, C. D., Lee, V. M. Y.,
918 George, J. M., and Rienstra, C. M. (2016) Solid-state NMR structure of a
919 pathogenic fibril of full-length human α -synuclein. *Nat. Struct. Mol. Biol.*
920 23, 409–415.
- 921 (27) Tóth, G., Gardai, S. J., Zago, W., Bertocini, C. W., Cremades, N.,
922 Roy, S. L., Tambe, M. A., Rochet, J.-C., Galvagnion, C., Skibinski, G.,
923 Finkbeiner, S., Bova, M., Regnstrom, K., Chiou, S.-S., Johnston, J.,
924 Callaway, K., Anderson, J. P., Jobling, M. F., Buell, A. K., Yednock, T. A.,
925 Knowles, T. P. J., Vendruscolo, M., Christodoulou, J., Dobson, C. M.,
926 Schenk, D., and McConlogue, L. (2014) Targeting the intrinsically
927 disordered structural ensemble of α -synuclein by small molecules as a
928 potential therapeutic strategy for Parkinson's disease. *PLoS One* 9,
929 e87133–11.
- 930 (28) Kakish, J., Lee, D., and Lee, J. S. (2015) Drugs which bind to
931 alpha-synuclein. Neuroprotective or neurotoxic? *ACS Chem. Neurosci.* 6
932 (12), 1930–40.
- 933 (29) Perni, M., Galvagnion, C., Maltsev, A., Meisl, G., Muller, M. B. D.,
934 Challa, P. K., Kirkegaard, J. B., Flagmeier, P., Cohen, S. I. A., Cascella, R.,
935 Chen, S. W., Limboker, R., Sormanni, P., Heller, G. T., Aprile, F. A.,
936 Cremades, N., Cecchi, C., Chiti, F., Nollen, E. A. A., Knowles, T. P. J.,
937 Vendruscolo, M., Bax, A., Zaslhoff, M., and Dobson, C. M. (2017) A
938 natural product inhibits the initiation of α -synuclein aggregation and
939 suppresses its toxicity. *Proc. Natl. Acad. Sci. U. S. A.* 114 (6), E1009–
940 E1017.
- 941 (30) Galvagnion, C., Brown, J. W. P., Oubrai, M. M., Flagmeier, P.,
942 Vendruscolo, M., Buell, A. K., Sparr, E., and Dobson, C. M. (2016)
943 Chemical properties of lipids strongly affect the kinetics of the
944 membrane-induced aggregation of α -synuclein. *Proc. Natl. Acad. Sci.*
945 *U. S. A.* 113, 7065–7070.
- 946 (31) Zaslhoff, M., Williams, J. I., Chen, Q., Anderson, M., Maeder, T.,
947 Holroyd, K., Jones, S., Kinney, W., Cheshire, K., and McLane, M. (2001)
948 A spermine-coupled cholesterol metabolite from the shark with potent
949 appetite suppressant and antidiabetic properties. *Int. J. Obes.* 25, 689–
950 697.
- (32) Zaslhoff, M., Adams, A. P., Beckerman, B., Campbell, A., Han, Z.,
Luijten, E., Meza, I., Julander, J., Mishra, A., Qu, W., Taylor, J. M.,
Weaver, S. C., and Wong, G. C. L. (2011) Squalamine as a broad-
spectrum systemic antiviral agent with therapeutic potential. *Proc. Natl.*
Acad. Sci. U. S. A. 108, 15978–15983.
- (33) Rao, M. N., Shinnar, A. E., Noecker, L. A., Chao, T. L., Feibush, B.,
Snyder, B., Sharkansky, I., Sarkahian, A., Zhang, X., Jones, S. R., Kinney,
W. A., and Zaslhoff, M. (2000) Aminosterols from the Dogfish Shark
Squalus acanthias. *J. Nat. Prod.* 63, 631–635.
- (34) Sills, A. K., Williams, J. I., Tyler, B. M., Epstein, D. S., Sipos, E. P.,
Davis, J. D., McLane, M. P., Pitchford, S., Cheshire, K., Gannon, F. H.,
Kinney, W. A., Chao, T. L., Donowitz, M., Lartera, J., Zaslhoff, M., and
Brem, H. (1998) Squalamine inhibits angiogenesis and solid tumor
growth in vivo and perturbs embryonic vasculature. *Cancer Res.* 58,
2784–2792.
- (35) Krishnan, N., Koveal, D., Miller, D. H., Xue, B., Akshinthala, S. D.,
Kragelj, J., Jensen, M. R., Gauss, C.-M., Page, R., Blackledge, M.,
Muthuswamy, S. K., Peti, W., and Tonks, N. K. (2014) Targeting the
disordered C terminus of PTP1B with an allosteric inhibitor. *Nat. Chem.*
Biol. 10, 558–566.
- (36) Qin, Z., Pandey, N. R., Zhou, X., Stewart, C. A., Hari, A., Huang,
H., Stewart, A. F. R., Brunel, J. M., and Chen, H.-H. (2015) Functional
properties of Claramine: a novel PTP1B inhibitor and insulin-mimetic
compound. *Biochem. Biophys. Res. Commun.* 458, 21–27.
- (37) Lantz, K. A., Hart, S. G. E., Planey, S. L., Roitman, M. F., Ruiz-
White, I. A., Wolfe, H. R., and McLane, M. P. (2010) Inhibition of
PTP1B by Trodusquemine (MSI-1436) Causes Fat-specific Weight
Loss in Diet-induced Obese Mice. *Obesity* 18, 1516–1523.
- (38) Ahima, R. S., Patel, H. R., Takahashi, N., Qi, Y., Hileman, S. M.,
and Zaslhoff, M. A. (2002) Appetite suppression and weight reduction by
a centrally active aminosterol. *Diabetes* 51, 2099–2104.
- (39) Smith, A. M., Maguire-Nguyen, K. K., Rando, T. A., Zaslhoff, M. A.,
Strange, K. B., and Yin, V. P. (2017) The protein tyrosine phosphatase
1B inhibitor MSI-1436 stimulates regeneration of heart and multiple
other tissues. *NPJ. Regen. Med.* 2, 57.
- (40) Yeung, T., Gilbert, G. E., Shi, J., Silvius, J., Kapus, A., and
Grinstein, S. (2008) Membrane Phosphatidyserine Regulates Surface
Charge and Protein Localization. *Science* 319, 210–212.
- (41) Brown, J. W. P., Buell, A. K., Michaels, T. C. T., Meisl, G., Carozza,
J., Flagmeier, P., Vendruscolo, M., Knowles, T. P. J., Dobson, C. M., and
Galvagnion, C. (2016) β -Synuclein suppresses both the initiation and
amplification steps of α -synuclein aggregation via competitive binding
to surfaces. *Sci. Rep.* 6, 36010.
- (42) Gaspar, R., Meisl, G., Buell, A. K., Young, L., Kaminski, C. F.,
Knowles, T. P. J., Sparr, E., and Linse, S. (2017) Acceleration of α -
synuclein aggregation. *Amyloid* 24, 20–21.
- (43) Fusco, G., Pape, T., Stephens, A. D., Mahou, P., Costa, A. R.,
Kaminski, C. F., Kaminski Schierle, G. S., Vendruscolo, M., Veglia, G.,
Dobson, C. M., and De Simone, A. (2016) Structural basis of synaptic
vesicle assembly promoted by α -synuclein. *Nat. Commun.* 7, 12563.
- (44) Cohen, S. I. A., Arosio, P., Presto, J., Kurudenkandy, F. R.,
Biverstal, H., Dolfe, L., Dunning, C., Yang, X., Frohm, B., Vendruscolo,
M., Johansson, J., Dobson, C. M., Fisahn, A., Knowles, T. P. J., and Linse,
S. (2015) The molecular chaperone Brichos breaks the catalytic cycle
that generates toxic $A\beta$ oligomers. *Nat. Struct. Mol. Biol.* 22, 207–213.
- (45) Seidler, J., McGovern, S. L., Doman, T. N., and Shoichet, B. K.
(2003) Identification and Prediction of Promiscuous Aggregating
Inhibitors among Known Drugs. *J. Med. Chem.* 46, 4477–4486.
- (46) Cremades, N., Cohen, S. I. A., Deas, E., Abramov, A. Y., Chen, A.
Y., Orte, A., Sandal, M., Clarke, R. W., Dunne, P., Aprile, F. A.,
Bertocini, C. W., Wood, N. W., Knowles, T. P. J., Dobson, C. M., and
Klenerman, D. (2012) Direct observation of the interconversion of
normal and toxic forms of α -synuclein. *Cell* 149, 1048–1059.
- (47) Chen, S. W., Drakulic, S., Deas, E., Oubrai, M., Aprile, F. A.,
Arranz, R., Ness, S., Roodveldt, C., Guillems, T., De-Genst, E. J.,
Klenerman, D., Wood, N. W., Knowles, T. P. J., Alfonso, C., Rivas, G.,
Abramov, A. Y., Valpuesta, J. M., Dobson, C. M., and Cremades, N.
(2015) Structural characterization of toxic oligomers that are kinetically

- 1019 trapped during α -synuclein fibril formation. *Proc. Natl. Acad. Sci. U. S. A.*
1020 *112*, E1994–2003.
- 1021 (48) Chen, S. W., Drakulic, S., Deas, E., Ouberai, M., Aprile, F. A.,
1022 Arranz, R., Ness, S., Roodveldt, C., Guilliams, T., De-Genst, E. J.,
1023 Klenerman, D., Wood, N. W., Knowles, T. P. J., Alfonso, C., Rivas, G.,
1024 Abramov, A. Y., Valpuesta, J. M., Dobson, C. M., and Cremades, N.
1025 (2015) Structural characterization of toxic oligomers that are kinetically
1026 trapped during α -synuclein fibril formation. *Proc. Natl. Acad. Sci. U. S. A.*
1027 *112*, E1994–E2003.
- 1028 (49) Flagmeier, P., De, S., Wirthensohn, D. C., Lee, S. F., Vincke, C.,
1029 Muyldermans, S., Knowles, T. P. J., Gandhi, S., Dobson, C. M., and
1030 Klenerman, D. (2017) Ultrasensitive Measurement of Ca (2+) Influx
1031 into Lipid Vesicles Induced by Protein Aggregates. *Angew. Chem., Int. Ed.*
1032 *56*, 7750–7754.
- 1033 (50) Evangelisti, E., Cascella, R., Becatti, M., Marrazza, G., Dobson, C.
1034 M., Chiti, F., Stefani, M., and Cecchi, C. (2016) Binding affinity of
1035 amyloid oligomers to cellular membranes is a generic indicator of
1036 cellular dysfunction in protein misfolding diseases. *Sci. Rep.* *6*, 32721.
- 1037 (51) Eisenberg, T., Knauer, H., Schauer, A., Büttner, S., Ruckenstein,
1038 C., Carmona-Gutierrez, D., Ring, J., Schroeder, S., Magnes, C.,
1039 Antonacci, L., Fussi, H., Deszcz, L., Hartl, R., Schraml, E., Criollo, A.,
1040 Megalou, E., Weiskopf, D., Laun, P., Heeren, G., Breitenbach, M.,
1041 Grubeck-Loebenstein, B., Herker, E., Fahrenkrog, B., Fröhlich, K.-U.,
1042 Sinner, F., Tavernarakis, N., Minois, N., Kroemer, G., and Madeo, F.
1043 (2009) Induction of autophagy by spermidine promotes longevity. *Nat.*
1044 *Cell Biol.* *11*, 1305–1314.
- 1045 (52) Bauer, J. H., Morris, S. N. S., Chang, C., Flatt, T., Wood, J. G., and
1046 Helfand, S. L. (2008) dSir2 and Dmp53 interact to mediate aspects of
1047 CR-dependent life span extension in *D. melanogaster*. *Aging* *1*, 38–48.
- 1048 (53) Hamilton, B., Dong, Y., Shindo, M., Liu, W., Odell, I., Ruvkun, G.,
1049 and Lee, S. S. (2005) A systematic RNAi screen for longevity genes in *C.*
1050 *elegans*. *Genes Dev.* *19*, 1544–1555.
- 1051 (54) Sarin, S., Prabhu, S., O'Meara, M. M., Pe'er, I., and Hobert, O.
1052 (2008) *Caenorhabditis elegans* mutant allele identification by whole-
1053 genome sequencing. *Nat. Methods* *5*, 865–867.
- 1054 (55) Kim, Y., and Sun, H. (2007) Functional genomic approach to
1055 identify novel genes involved in the regulation of oxidative stress
1056 resistance and animal lifespan. *Aging Cell* *6*, 489–503.
- 1057 (56) Dillin, A., Hsu, A.-L., Arantes-Oliveira, N., Lehrer-Graiwer, J.,
1058 Hsin, H., Fraser, A. G., Kamath, R. S., Ahringer, J., and Kenyon, C.
1059 (2002) Rates of behavior and aging specified by mitochondrial function
1060 during development. *Science* *298*, 2398–2401.
- 1061 (57) Lee, S. S., Kennedy, S., Tolonen, A. C., and Ruvkun, G. (2003)
1062 DAF-16 target genes that control *C. elegans* life-span and metabolism.
1063 *Science* *300*, 644–647.
- 1064 (58) Jorgensen, E. M., and Mango, S. E. (2002) The art and design of
1065 genetic screens: *Caenorhabditis elegans*. *Nat. Rev. Genet.* *3*, 356–369.
- 1066 (59) Ayyavevara, S., Balasubramaniam, M., Johnson, J., Alla, R.,
1067 Mackintosh, S. G., and Reis, R. J. S. (2016) PIP(3)-binding proteins
1068 promote age-dependent protein aggregation and limit survival in *C.*
1069 *elegans*. *Oncotarget* *7*, 48870–48886.
- 1070 (60) Johnson, C. S. (1999) Diffusion ordered nuclear magnetic
1071 resonance spectroscopy: Principles and applications. *Prog. Nucl. Magn.*
1072 *Reson. Spectrosc.* *34*, 203–256.
- 1073 (61) Wu, D. H., Chen, A. D., and Johnson, C. S. (1995) An Improved
1074 Diffusion-Ordered Spectroscopy Experiment Incorporating Bipolar-
1075 Gradient Pulses. *J. Magn. Reson., Ser. A* *115*, 260–264.
- 1076 (62) Stejskal, E. O., and Tanner, J. E. (1965) Spin Diffusion
1077 Measurements: Spin Echoes in the Presence of a Time-Dependent
1078 Field Gradient. *J. Chem. Phys.* *42*, 288–292.
- 1079 (63) Capitini, C., Conti, S., Perni, M., Guidi, F., Cascella, R., De Poli,
1080 A., Penco, A., Relini, A., Cecchi, C., and Chiti, F. (2014) TDP-43
1081 inclusion bodies formed in bacteria are structurally amorphous, non-
1082 amyloid and inherently toxic to neuroblastoma cells. *PLoS One* *9*,
1083 e86720.
- 1084 (64) Di Natale, C., Scognamiglio, P. L., Cascella, R., Cecchi, C., Russo,
1085 A., Leone, M., Penco, A., Relini, A., Federici, L., Di Matteo, A., Chiti, F.,
1086 Vitagliano, L., and Marasco, D. (2015) Nucleophosmin contains
amyloidogenic regions that are able to form toxic aggregates under
physiological conditions. *FASEB J.* *29*, 3689–3701.
- (65) Brenner, S. (1974) The genetics of *Caenorhabditis elegans*.
Genetics *77*, 71–94.
- (66) Van Ham, T. J., Thijssen, K. L., Breitling, R., Hofstra, R. M. W.,
Plasterk, R. H. A., and Nollen, E. A. A. (2008) *C. elegans* model
identifies genetic modifiers of α -synuclein inclusion formation during
aging. *PLoS Genet.* *4*, e1000027–11.
- (67) Perni, M., Challa, P. K., Kirkegaard, J. B., Limbocker, R.,
Koopman, M., Hardenberg, M. C., Sormanni, P., Müller, T., Saar, K. L.,
Roode, L. W. Y., Habchi, J., Vecchi, G., Fernando, N. W., Casford, S.,
Nollen, E. A. A., Vendruscolo, M., Dobson, C. M., and Knowles, T. P. J.
(2018) Massively parallel *C. elegans* tracking provides multi-dimen-
sional fingerprints for phenotypic discovery. *J. Neurosci. Methods*,
DOI: 10.1016/j.jneumeth.2018.02.005.
- (68) Van der Goot, A. T., Zhu, W., Vazquez-Manrique, R. P., Seinstra,
R. I., Dettmer, K., Michels, H., Farina, F., Krijnen, J., Melki, R., Buijsman,
R. C., Ruiz Silva, M., Thijssen, K. L., Kema, I. P., Neri, C., Oefner, P. J.,
and Nollen, E. A. A. (2012) Delaying aging and the aging-associated
decline in protein homeostasis by inhibition of tryptophan degradation.
Proc. Natl. Acad. Sci. U. S. A. *109*, 14912–14917.